

# Wideband Inline-amplified WDM Transmission Using PPLN-based OPA with Over-10-THz Bandwidth

T. Kobayashi<sup>1</sup>, S. Shimizu<sup>1</sup>, M. Nakamura<sup>1</sup>, T. Umeki<sup>1,2</sup>, T. Kazama<sup>2</sup>, R. Kasahara<sup>2</sup>,  
F. Hamaoka<sup>1</sup>, M. Nagatani<sup>1,2</sup>, H. Yamazaki<sup>1,2</sup>, T. Mizuno<sup>1</sup>, H. Nosaka<sup>1,2</sup> and Y. Miyamoto<sup>1</sup>

1: NTT Network Innovation Laboratories, 1-1 Hikari-no-oka, Yokosuka, Kanagawa, Japan

2: NTT Device Technology Laboratories, 3-1 Morinosato Wakamiya, Atsugi, Kanagawa, Japan

Email: takayuki.kobayashi.wt@hco.ntt.co.jp

**Abstract:** We demonstrate the first inline-amplified transmission with PPLN-based polarization-independent OPA offering 5.125-THz amplification bandwidth and  $\geq 15$ -dB gain using 800-Gb/s PDM PS-36QAM signals. Results indicate the OPA potentially extends the WDM bandwidth to over 10.25 THz. © 2020 The Author(s)

## 1. Introduction

According to the Shannon-theorem, increasing the signal bandwidth is important for increasing the capacity of optical transmission systems without the requirement of a higher signal-to-noise-ratio (SNR) to maintain backward compatibility of transmission distance. Extension of the optical amplification bandwidth is attractive to extend the capacity by replacing optical repeaters at the deployed-fiber link. Digital-coherent transmission experiments involving the use of optical bandwidth over 10-THz have been conducted based on hybrid Raman/EDFAs [1, 2], all-Raman amplification [3], or extra optical band utilization such as S-, C- and L-bands [4, 5]. In addition, a semiconductor optical amplifier with over-100-nm continuous bandwidth was developed and demonstrated [6]. Optical parametric amplification is an alternative technique and have been studied using highly-nonlinear fibers or periodically poled LiNbO<sub>3</sub> (PPLN) waveguides [7, 8]. The attractive features of an optical parametric amplifier (OPA) are little gain-transient effect, wide band [9, 10] and high gain [11, 12], and has applications such as spectral-inversion and phase-sensitive amplification for improving the SNR after transmission. However, few studies have demonstrated transmission with fiber-based OPA as a phase-insensitive inline-amplifier in the cases of single channel [13] and a small number of WDM channels [14]. Thus, wide-band inline-amplified WDM transmission using a phase-insensitive OPA which is beyond standard EDFA bandwidth of 4 THz has also not yet been reported.

In this paper, we demonstrate for the first time that inline-amplified WDM transmission over low-loss G.654.E fiber with a PPLN-based phase-insensitive OPA by using 41-ch 800-Gb/s polarization-division-multiplexed (PDM) probabilistically-shaped (PS)-36QAM signals within a 125-GHz-spaced WDM slot. High-conversion-efficient PPLN modules provide the over-10-THz amplification bandwidth, the gain of beyond 15 dB and the noise figure (NF) of less than 5.1-dB. A re-circulating transmission repeating three 30.8-km spans confirms that a PPLN-based OPA as an inline-amplifier can potentially extended the amplification bandwidth to over 10 THz.

## 2. PPLN-based optical parametric amplifier with > 10-THz bandwidth

Figure 1(a) shows the conceptual configuration of a polarization-independent OPA with over-10-THz bandwidth using high-conversion-efficient and wide-band PPLN modules [15]. In this OPA, longer wavelength band and shorter wavelength band are separately amplified after band-dividing filter. Two sets of the OPAs are required for achieving an amplification bandwidth of 10-THz. The second-harmonic-pumping scheme is used because it can provide the amplification without the undesired optical parametric process [16]. The PPLN modules (PPLN 1 & 2) are used to achieve parametric amplification of polarization tributaries by difference frequency generation (DFG). The additional PPLN modules are used to generate pump lights for DFG via second harmonic generation (SHG). An external-cavity laser (ECL) with 5-kHz linewidth is used as the fundamental light source for SHG; its wavelength  $\lambda_F$  is 1545.32 nm (194 THz). The input WDM signal is divided into two polarization tributaries by using a polarization beam splitter (PBS), and fed into a PPLN module at each polarization lane. After parametric amplification by DFG, the amplified

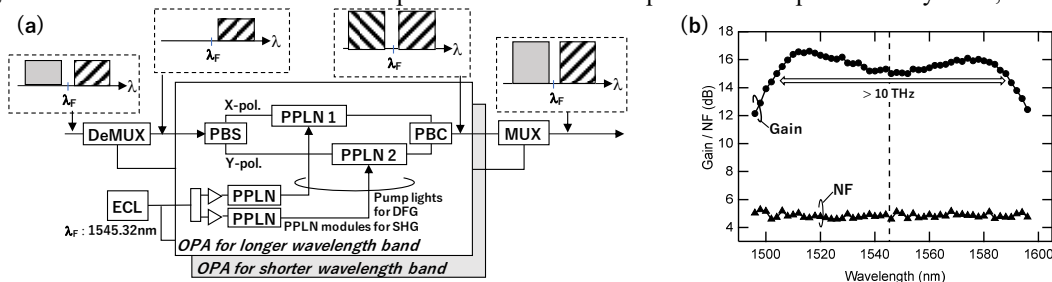


Fig.1 (a) Configuration of PPLN-based polarization-independent OPA; (b) Gain and NF spectra w/o MUX/DeMUX filters

signals attached with the idler of both polarization components are combined using a polarization beam combiner (PBC). Finally, the two amplified bands are combined while rejecting the unnecessary idler by a multiplexing-filter. The gain and NF of the OPA excluding the losses of MUX/DeMUX filters are shown in Fig.1 (b). It is measured at the output of the PBC by sweeping the wavelength of CW light with the input power of  $-25$  dBm. The pumping power to each PPLN-module for SHG is set to  $\sim 2$  W. 125-GHz guard-band was inserted around the fundamental light wavelength of 1545.32 nm because a signal crossing the fundamental wavelength is not properly amplified. At the wavelength range of 1504 to 1588 nm, the 10.2-THz amplification bandwidth, over-15-dB gain and flat NF spectra around 5 dB are achieved. We implemented a set of the OPA enclosed in a box in Fig.1(a) for the transmission experiment.

### 3. Experimental setup

Figure 2 shows the experimental setup. A Nyquist-pulse-shaped 120-Gbaud PS-36QAM signal was generated using an IQ-modulator driven by bandwidth-doubler-based high-speed DACs [17]. The 64QAM was truncated to 36QAM for PAPR reduction, and the symbol distribution was probabilistically shaped to a Maxwell-Boltzmann distribution for achieving the target information rate of 4.435. We used the concatenated code of LDPC and BCH with a code rate of 0.826. Assuming 1.64% pilot-signal insertion, a net data rate of a 120-Gbaud PS-36QAM signal after PDM by using a PDM emulator (PDME) was 800 Gb/s  $[2 \times \{4.4375 - (1 - 0.826) \times 6\} / 1.0164 \times 120 \text{ Gbaud}]$  [18]. To emulate a 41-channel 125-GHz-spaced WDM signal, amplified spontaneous emission (ASE) was loaded to the 5.125-THz optical band from 1505.55 to 1587.25 nm except the wavelength of the measurement signal [19]. ASE with flat and broadband spectra was achieved by coupling using a 3-dB coupler after spectral shaping of the EDFA output with optical gain equalizer at each C- and L-band. The measurement signal was coupled with the interfering WDM signal using a 3-dB coupler, then the WDM signal was fed into the re-circulating loop.

The transmission line consisted of a re-circulating loop containing a 30.8-km G.654.E fiber with a  $125\text{-}\mu\text{m}^2$  effective area, loop-synchronous polarization scrambler (LSPS), optical switches (SWs), a wavelength blocker and the 1-stage OPA. The OPA with 15-dB gain further compensated for the losses of the transmission fiber (5.6 dB at 1550 nm), the wavelength blocker (5.5 dB) and other loop components. Transmission fiber length in the loop was mainly limited by the insertion loss of wavelength blocker. The WDM signal at each point, (A), (B) and (C) is shown on the right of Fig.2. 10.25-THz WDM signal was fed into the transmission fiber at each loop after the parametric amplification of the input signal, and the 41 shorter-wavelength channels were continuously re-circulated in the loop. In the 1st loop, the OPA as a post-amplifier amplified the 5.125-THz WDM signal resulting in a 10.25-THz WDM signal containing the amplified WDM signal and its idler. In 2<sup>nd</sup> loop and following loops, the wavelength blocker suppressed the longer-wavelength signals compared to the fundamental light of 1545.32 nm and the 41 shorter-wavelength signals were input to the OPA as an inline-amplifier. Because of the limitation in the number of PPLN modules, the amplification bandwidth was restricted to half the ideal configuration of the OPA. As a result, the 10.25-THz WDM signal was fed into the transmission fiber.

At the receiver side, the measurement signal was amplified with an S-, C- or L-band rare-earth-doped fiber amplifier and extracted using a tunable optical bandpass filter. The received signal was digitized using a digital storage oscilloscope operated at 200 GS/s with 70-GHz bandwidth and post-processed off-line with a complex  $8 \times 2$  MIMO equalizer [20]. Bit wise log-likelihood ratios (LLRs) were calculated by bit-metric decoding applied to each recovered symbol. Finally, the normalized generalized mutual information (NGMI) for the PS-36QAM was computed with the LLRs. The NGMI threshold of the outer BCH code was 0.857 [20].

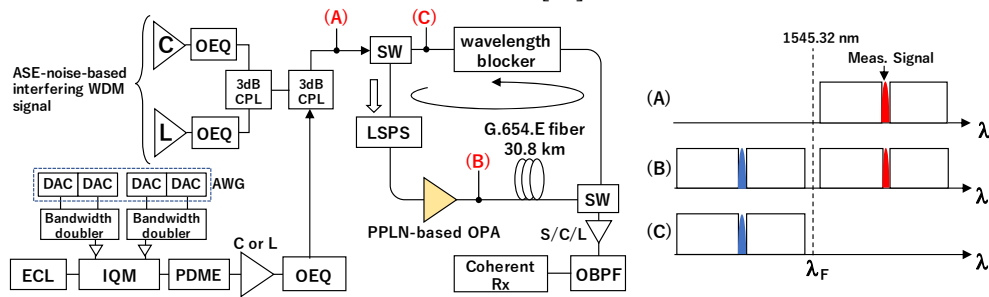


Fig.2 Experimental setup, and optical spectra at the point, (A), (B) and (C)

### 4. Results

We first measured the input power causing gain saturation in a back-to-back configuration. A 5.125-THz WDM signal or single channel was input to an OPA, and the total input power was varied from  $-9$  to 7 dBm in 2-dB increments. As shown in Fig.3(a), the gradual gain saturation was observed in the both cases of single channel and WDM. No nonlinear distortion on the signals was observed at the higher input-power region as the constellation diagrams shown

in the inset of the Fig.3(a). We used the total input power of  $-5$  dBm in the transmission experiments. It corresponds to an averaged channel power of  $-21$  dBm in the 41-channel WDM configuration. Averaged fiber input power was  $-6$  dBm/ch. Regarding the dependency of amplified-signal quality on the bandwidth of an input WDM signal after  $3 \times 30.8$ -km transmission as shown in Fig.3(b), the input-signal bandwidth was varied by adding an interfering WDM signal of 1.875-THz in the C-band, 2.625-THz in the L-band, or 5.125-THz full loading to the measurement signal at a wavelength of 1537.4 nm. This corresponds to changing the number of WDM channels to 1, 16, 22, and 41. Under each condition, significant degradation in the NGMI was not observed. This indicates dynamic range of the OPA's input power is at least 16 dB. Finally, we conducted all-channel measurement at  $3 \times 30.8$  km. Figure 4(a) shows the optical spectra at the input of the loop and the output of the fiber at each loop. The maximum number of loops was set to 3 because there was no gain equalizer in the loop to maintain the flatness of the WDM signal. The NGMI of all channels after 92.4-km transmission is shown in Fig.4(b). The NGMI of all 41 channels in each optical band is better than the threshold of 0.857 represented with a dashed line. Figure 4(c) shows the stability of both polarization amplifications was achieved after 100 NGMI measurements. These results indicate that 5.125-THz inline-amplified transmission with a PPLN-based OPA was successfully demonstrated, and amplification bandwidth can be potentially extended to 10.25 THz by measuring the signal quality of both signals and idlers.

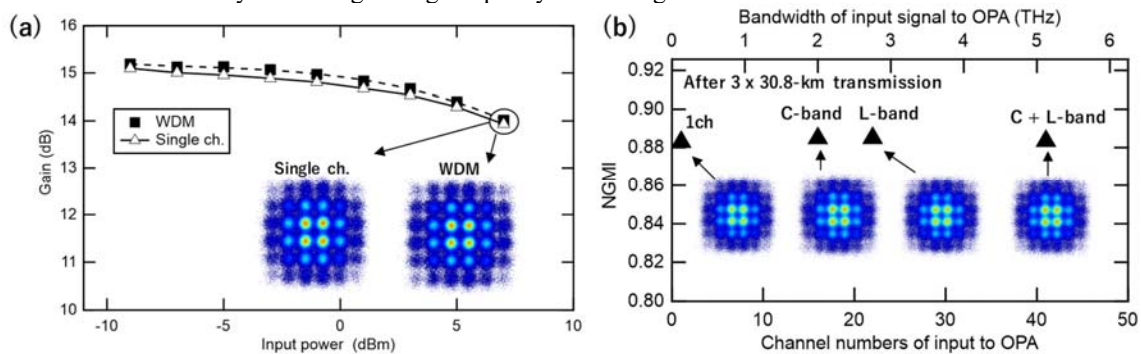


Fig. 3 OPA characteristics: (a) Gain saturation and (b) dependency of amplified-signal quality on input-signal bandwidth

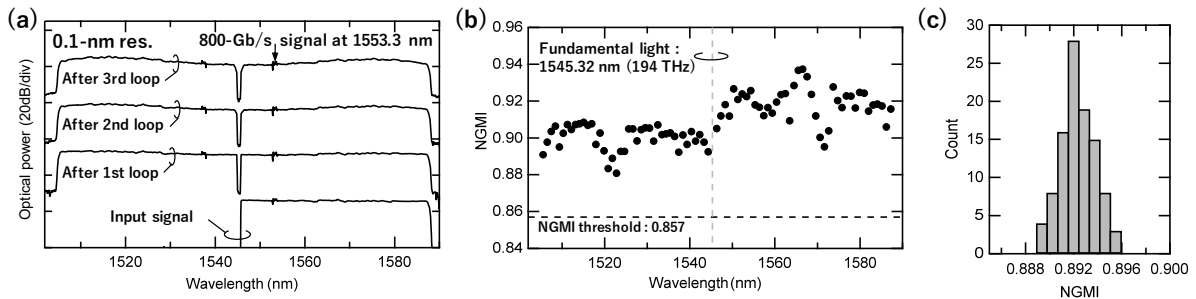


Fig. 4 Inline-amplified WDM transmission results over G.654.E fiber with 800-Gb/s/λ PS-36QAM signals:

- (a) Optical spectra at output of fiber at each loop, (b) NGMIs of WDM channels after 92.4-km ( $3 \times 30.8$  km) transmission, (c) NGMI variance in wavelength of 1537.4 nm after 92.4-km transmission

#### 4. Conclusion

We successfully demonstrated the first inline-amplified WDM transmission with a PPLN-based OPA using 125-GHz-spaced 800-Gb/s PS-36QAM signals over 92.4-km G.654.E fiber. The PPLN-based polarization-independent OPA provides a 5.125-THz amplification bandwidth with more than 15-dB gain. We have also shown the PPLN-based OPA can potentially extend the amplification bandwidth to over 10 THz.

#### 5. References

- [1] H. Masuda et al., in Proc. OFC2007, paper PDP20, 2007.
- [2] M. Ionescu et al., in Proc. ECOC2018, paper Mo4G.2., 2018.
- [3] A. Sano et al., in Proc. OFC2012, Paper PDP5C.3., 2012
- [4] F. Hamaoka et al., in Proc. ECOC2018, paper Mo4G.1., 2018.
- [5] T. Kato et al., in Proc. ECOC2019, paper PD.1.7, 2019.
- [6] J. Renaudier et al., in Proc. ECOC2017, paper Th.PDP.A.2., 2017.
- [7] M. E. Marhic, et al., Opt. Lett., vol. 21, p. 573, 1996.
- [8] Katia Gallo and Gaetano Assanto, Appl. Phys. Lett. 71, 1020, 1997.
- [9] T. Torounidis and P. Andrekson, IEEE Photon. Technol. Lett., 19(9), pp. 650-652, 2007.
- [10] J. Yamawaku et al., IEEE J. Sel Top Quantum Electron, vol. 12, no. 4, pp. 521-528, 2006.
- [11] T. Torounidis et al., IEEE Photon. Technol. Lett., 18(10), pp. 1194-1196, 2006.
- [12] T. Kashiwazaki et al., in Proc. NLO2019, paper NW3A.2, 2019.
- [13] Z. Lali-Dastjerdi et al., in Proc. ECOC2012, paper Mo.2.C.5, 2012.
- [14] M. F. C. Stephens et al., Optics express, 25(20), pp. 24312-24325, 2017.
- [15] T. Umeki et al., IEEE J. Quantum Electron. 46(8), 1206-1213, 2010.
- [16] T. Kazama et al., in Proc. OFC2016, paper M3D.1, 2016.
- [17] F. Hamaoka et al., in Proc. OFC2019, paper M2H.6, 2019.
- [18] M. Nakamura et al., in Proc. OFC2020, paper M4K.3, 2020.
- [19] D. J. Elson et al., Opt. Exp., vol. 25(16), pp. 19529-19537, 2017.
- [20] T. Kobayashi et al., in Proc. OFC2019, paper Th4B.2, 2019.